Cell

The Classical Complement Cascade Mediates CNS Synapse Elimination

Beth Stevens,[1,*] Nicola J. Allen,[1] Luis E. Vazquez,[1] Gareth R. Howell,[3,4] Karen S. Christopherson,[1] Navid Nouri,[1] Kristina D. Micheva,[2] Adrienne K. Mehalow,[3,4] Andrew D. Huberman,[1] Benjamin Stafford,[5] Alexander Sher,[5] Alan M. Litke,[5] John D. Lambris,[6] Stephen J. Smith,[2] Simon W.M. John,[3,4] and Ben A. Barres[1]
[1]Department of Neurobiology
[2]Department of Molecular and Cellular Physiology
[3]Stanford University School of Medicine, Stanford, CA 94305, USA
Howard Hughes Medical Institute
[4]The Jackson Laboratory, Bar Harbor, ME 04609, USA
[5]Santa Cruz Institute for Particle Physics, University of California, Santa Cruz, Santa Cruz, CA 95064, USA
[6]Department of Pathology and Laboratory Medicine, University of Pennsylvania Medical School, Pennsylvania, PA 19104, USA
*Correspondence: beths@stanfordmedalumni.org
DOI 10.1016/j.cell.2007.10.036

SUMMARY

During development, the formation of mature neural circuits requires the selective elimination of inappropriate synaptic connections. Here we show that C1q, the initiating protein in the classical complement cascade, is expressed by postnatal neurons in response to immature astrocytes and is localized to synapses throughout the postnatal CNS and retina. Mice deficient in complement protein C1q or the downstream complement protein C3 exhibit large sustained defects in CNS synapse elimination, as shown by the failure of anatomical refinement of retinogeniculate connections and the retention of excess retinal innervation by lateral geniculate neurons. Neuronal C1q is normally downregulated in the adult CNS; however, in a mouse model of glaucoma, C1q becomes upregulated and synaptically relocalized in the adult retina early in the disease. These findings support a model in which unwanted synapses are tagged by complement for elimination and suggest that complement-mediated synapse elimination may become aberrantly reactivated in neurodegenerative disease.

INTRODUCTION

The formation of mature neural circuits requires the activity-dependent pruning of inappropriate synapses (Katz and Shatz, 1996; Sanes and Lichtman, 1999; Hua and Smith, 2004), but the specific molecular mechanisms that drive synapse elimination are not known. The mouse retinogeniculate system has proven to be an excellent model system for studying developmental CNS synapse elimination (Jaubert-Miazza et al., 2005; Hooks and Chen, 2006). Axons from retinal ganglion cells (RGCs) terminate in distinct nonoverlapping eye-specific domains in the dorsal lateral geniculate nucleus (dLGN). The majority of eye-specific segregation occurs postnatally before the onset of vision, but synaptic pruning continues in monocular regions of the LGN during a 2 week period spanning eye opening (P8-P30 in mouse). Initially, dLGN neurons are multiply innervated by up to ten RGC axons, but by the third postnatal week, each dLGN neuron receives stable inputs from only one or two RGC axons (Hooks and Chen, 2006). This developmental shift in synaptic convergence represents the elimination of inappropriate retinogeniculate synapses and the maintenance and strengthening of appropriate synaptic connections. This dynamic period of synaptic refinement coincides with the appearance of astrocytes in the postnatal brain, and recent evidence indicates a role for astrocyte-derived signals in synapse development (Christopherson et al., 2005; Ullian et al., 2001).

Here we identify an unexpected role for astrocytes and the classical complement cascade in mediating CNS synapse elimination in the retinogeniculate pathway. By gene profiling, we found that all three chains of the complement protein C1q are strongly upregulated when purified RGCs are exposed to astrocytes. C1q is the initiating protein of the classical complement cascade, which is part of the innate immune system. When C1q binds to and coats (opsonizes) dead cells, pathogens, or debris, it triggers a protease cascade, leading to the deposition of the downstream complement protein C3 (Gasque, 2004). Opsonization with activated C3 fragments (C3b and iC3b) leads to cell or debris elimination in one of two ways. Deposited C3 can directly activate C3 receptors on macrophages or microglia, thereby triggering elimination by phagocytosis, or activated C3 can trigger the terminal activation of the complement cascade, leading to cell lysis through the formation of a lytic membrane attack complex. We show that complement proteins opsonize or

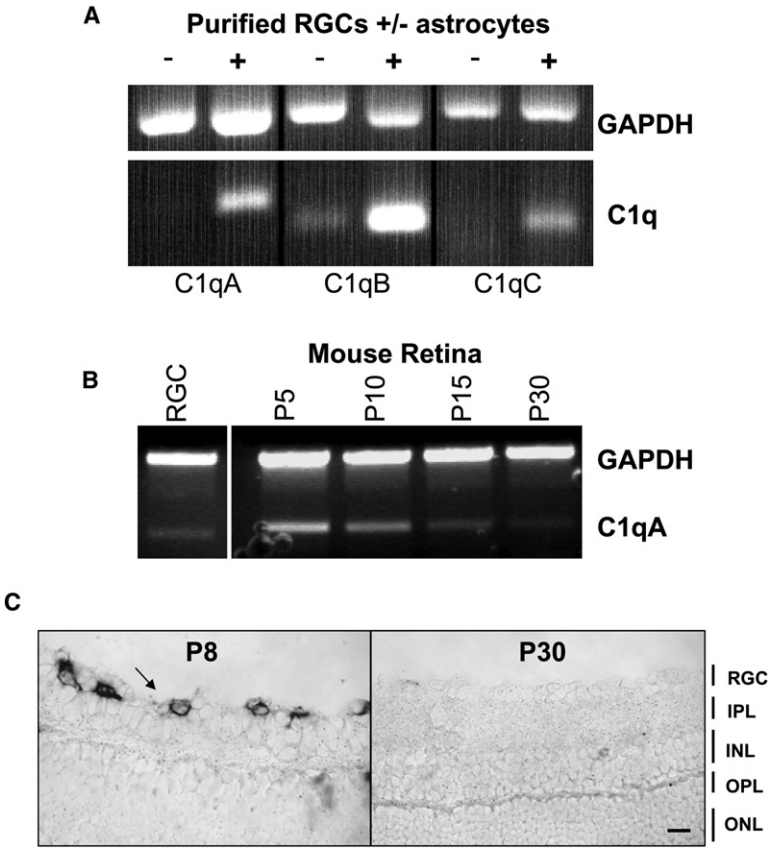

Figure 1. Astrocytes Upregulate C1q Expression by Neurons

(A) RT-PCR validation of our gene chip analysis confirms that astrocyte exposure upregulates mRNAs for all three chains (A, B, and C) of C1q in purified postnatal RGC neurons in culture.

(B) C1q is highly expressed by RGCs in vivo. RT-PCR analysis of mRNA isolated from RGCs that were acutely isolated from P5 retina (left lane) and PBS perfused whole postnatal mouse retina from different developmental time points (P5–P30).

(C) In situ hybridization confirmation that C1q is expressed by developing, but not mature, RGCs in vivo. Expression of C1qA was predominantly localized to retinal ganglion neurons (arrows) in fresh frozen sections of postnatal (P5) retina, but C1q gene expression was largely absent in RGCs by P30. RGC, retinal ganglion cell layer; IPL, inner plexiform layer; INL, inner nuclear layer; OPL, outer plexiform layer; ONL, outer nuclear layer. Scale bar, 20 μm.

"tag" CNS synapses during a discrete window of postnatal development and that the complement proteins C1q and C3 are required for synapse elimination in the developing retinogeniculate pathway. We also show that C1q becomes aberrantly upregulated and relocalized to adult retinal synapses in a mouse model of glaucoma at an early stage of the disease prior to overt neurodegeneration, suggesting that the complement cascade also mediates synapse loss in glaucoma and other CNS neurodegenerative diseases.

RESULTS

Astrocytes Upregulate All Three C1q Subunit mRNAs in Retinal Ganglion Cells

We used a gene profiling approach to screen candidate neuronal genes that are regulated by astrocytes. RNA was collected from purified postnatal RGCs that had been cultured for 1 week in the presence or absence of a feeding layer of cultured neonatally derived astrocytes, and the target RNA was hybridized to an Affymetrix gene chip. We found that mRNA for all three C1q chains was upregulated by astrocytes in purified RGCs by 10- to 30-fold, and we verified this upregulation using semiquantitative RT-PCR (Figure 1A). To confirm that C1q mRNA is normally expressed by developing RGCs in vivo, we performed RT-PCR analysis on mRNA collected from purified RGCs that were acutely isolated (Figure 1B) as well as in situ hybridization on whole retina (Figure 1C). We found that C1q mRNA levels were highest in postnatal RGCs between P5 and P10 and declined significantly by P30 (Figures 1B and 1C). Thus, C1q mRNA is expressed by RGCs in vitro in response to astrocytes and is normally expressed by postnatal, but not adult, RGCs in vivo during a window of development corresponding to the presence of immature astrocytes.

C1q Immunoreactivity Is Localized to Synapses throughout the Developing CNS

We next investigated whether C1q protein could be detected in the developing mouse CNS by immunostaining cryosections. Using several different C1q antisera, we observed bright, punctate C1q immunoreactivity throughout the developing retina that was enriched in the synaptic inner plexiform layer (IPL) of postnatal mouse retinas and was also observed in developing RGCs (Figure 2A). Consistent with the expression pattern of C1q mRNA in postnatal RGCs in vivo (Figure 1), C1q protein expression and synaptic localization followed a similar developmental pattern, being higher in the IPL at P5 and decreasing in the mature retina (Figure 2A). In addition, many C1q-positive puncta in the IPL were associated with synaptic puncta identified by double immunostaining with synaptic markers such as PSD-95 (Figure 2B). Together, these

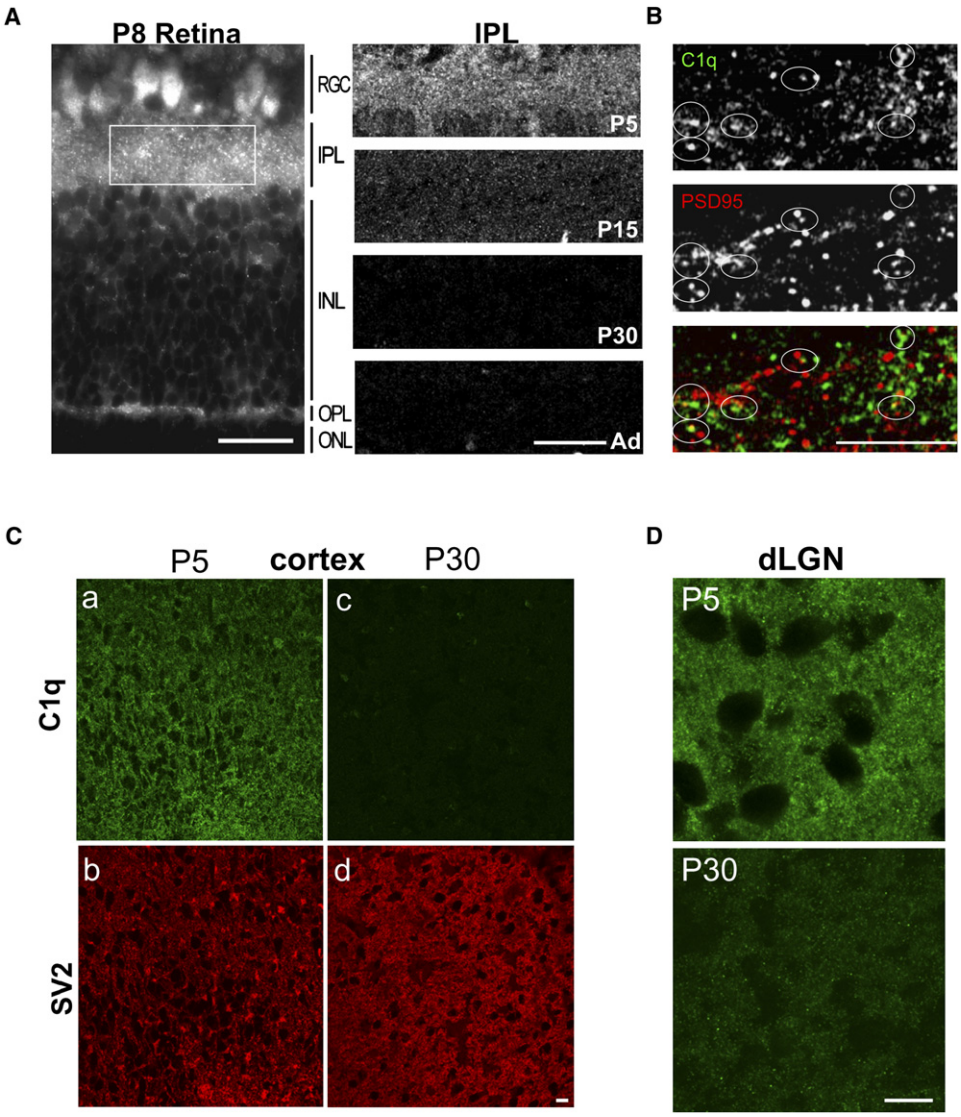

Figure 2. C1q Is Localized to Developing CNS Synapses In Vivo

(A) Longitudinal cryosection of a P8 mouse retina stained with anti-C1q. Layers of the retina are labeled on the right. Punctate C1q immunoreactivity is enriched in the synaptic inner plexiform layer (IPL). RGC, retinal ganglion cell layer; IPL, inner plexiform layer; INL, inner nuclear layer; OPL, outer plexiform layer; ONL, outer nuclear layer. Scale bar, 20 μm. Confocal imaging demonstrates the developmental enrichment of C1q in synaptic IPL of the mouse retina (panels, right). Zoomed-in images of IPL are from a region comparable to the boxed area in the epifluorescence image in panel (left). Punctate C1q immunoreactivity in the IPL was highest at P5 and largely decreased after P15. Scale bar, 20 μm.

(B) Double labeling of C1q (green) with the postsynaptic marker, PSD95 (red), demonstrates C1q-positive puncta in close proximity to PSD95 puncta in postnatal P5 retina. Several colocalized C1q and PSD95 puncta are highlighted (circles). Scale bar, 10 μm.

(C) Double immunohistochemistry with the synaptic antibody SV2 reveals a higher intensity of C1q immunoreactivity in synaptic regions of developing (Ca and Cb), but not the adult mouse cortex (Cc and Cd). Scale bar, 10 μm.

(D) Immunostaining of C1q (green) demonstrates strong punctate C1q immunoreactivity in the postnatal (P5) dLGN, but not the mature mouse dLGN (P30). Scale bar, 10 μm.

findings indicate that C1q protein is expressed by RGCs in vivo and that C1q is synaptically localized to the postnatal, but not mature, IPL.

To find out if C1q protein is also present in the brain, we next immunostained cryosections from postnatal and mature brain. We again observed punctate C1q staining in synaptic regions, particularly between P4 and P10, that closely resembled the pattern of immunoreactivity observed with synaptic markers such as SV2 (Figure 2C). Importantly, a similar expression pattern was observed in the postnatal dLGN, a major target of RGC axons (Figure 2D). As in the retina, synaptic C1q immunoreactivity in the cortex and LGN was developmentally downregulated (Figures 2C and 2D) and was largely absent when the

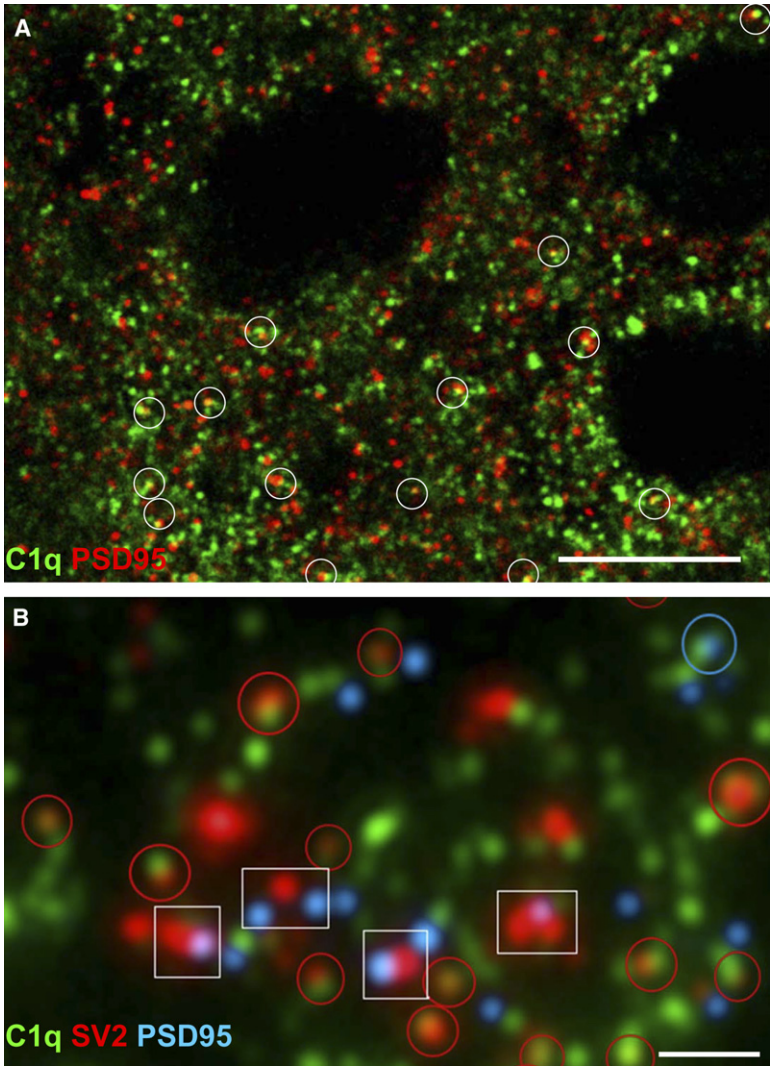

Figure 3. Synaptic Localization of C1q in the Developing LGN

(A) Single-plane confocal images of C1q (green) and PSD95 (red) revealed many C1q-positive puncta that colocalized with the postsynaptic protein, PSD95 in the developing dLGN (several examples are circled). Scale bar, 10 μm.

(B) Array tomography on 70 nm sections of LGN showing C1q (green), SV2 (red), and PSD-95 (blue) distribution in LGN. Synapses were defined by the close apposition of presynaptic (SV2) and postsynaptic (PSD-95) markers (white boxes). C1q was often colocalized with smaller SV2 and PSD95 synaptic puncta that lacked a synaptic partner. Several examples of C1q colocalization with SV2 (red circles) or PSD95 (blue circles) are highlighted. Scale bar, 2 μm.

antisera was preadsorbed with purified C1q protein (see Figure S1 available online). Thus, C1q immunoreactivity is localized to synapses throughout the postnatal, but not adult, brain and retina.

To further investigate the synaptic localization of C1q in the developing brain, we performed double immunostaining with antibodies to C1q and synaptic markers. Using confocal microscopy, we observed many C1q-positive puncta that colocalized with the postsynaptic protein PSD95 in the developing dLGN (Figure 3A). In order to better visualize C1q's synaptic localization, we turned to array tomography, a powerful new imaging technique that significantly improves the spatial resolution of closely apposed synaptic proteins over confocal microscopy (Micheva and Smith, 2007). We performed double and triple immunofluorescence for C1q, SV2, and PSD95 on ultrathin resin embedded serial sections of P8 dLGN (Figure 3B). Mature synapses were identified as closely apposed presynaptic (SV2-positive) and postsynaptic (PSD95-positive) puncta (Figure 3B, white boxes). We also observed smaller SV2 or PSD-95 puncta, which lacked a synaptic partner. These structures most probably represent immature synapses or synapses in the process of elimination. Interestingly, C1q was often colocalized with these smaller SV2 and PSD95 synaptic puncta (Figure 3B, circles), while large SV2-PSD95 synapses were not often closely associated with C1q. These findings suggest the possibility that C1q may be opsonizing immature synapses, or synapses that are being eliminated in the developing dLGN. Taken together, these experiments provide evidence that C1q is localized to synapses in the developing retina and brain during the period of synaptic pruning.

C1q Is Required for Retinogeniculate Refinement

The localization of C1q to developing synapses, together with C1q's known role in eliminating unwanted cells and debris, suggested a role for C1q in mediating synapse elimination. To test this hypothesis, we next used a combination of neuroanatomical and electrophysiological

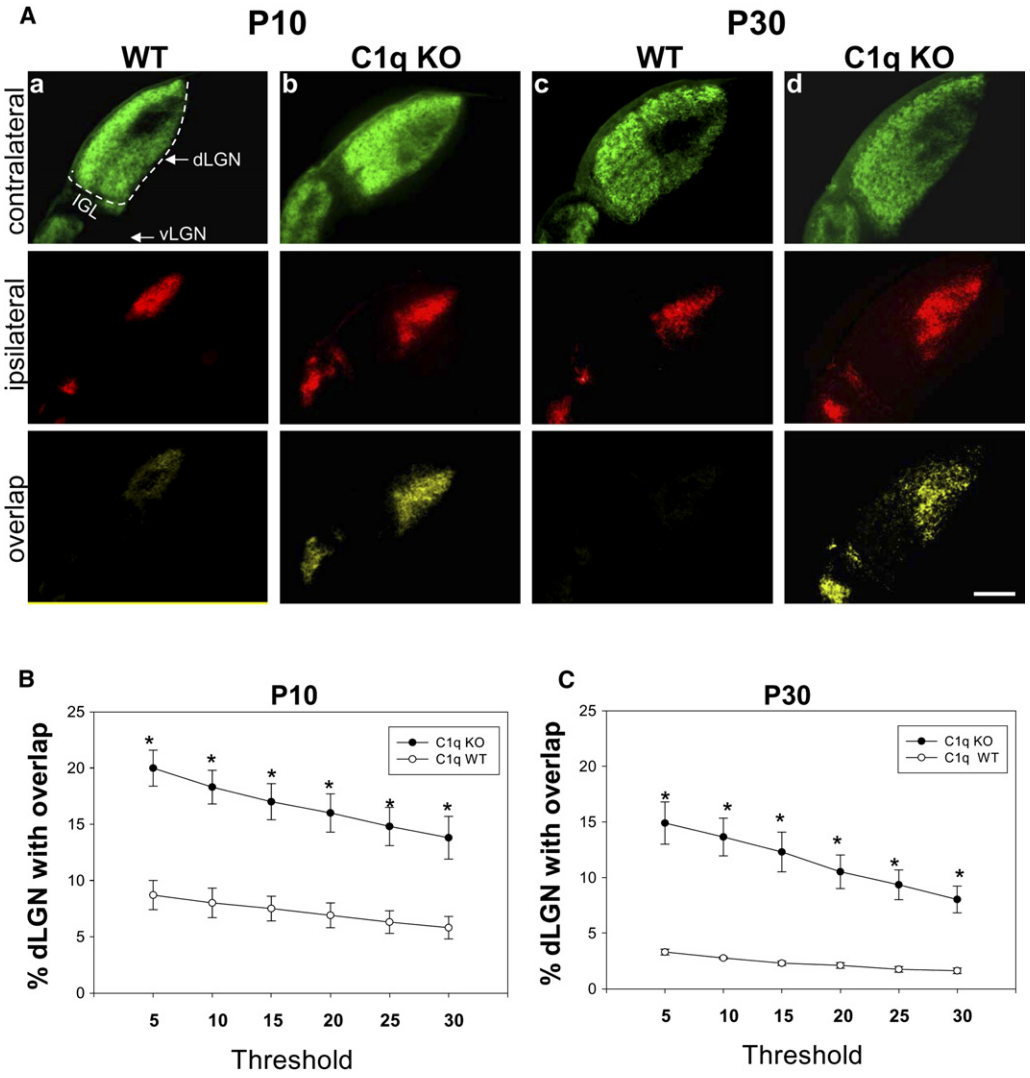

Figure 4. C1q-Deficient Mice Have Defects in Synaptic Refinement and Eye-Specific Segregation

(A) Retinogeniculate projection patterns visualized after injecting β-cholera toxin conjugated to Alexa 594 (CTβ-594) dye (red) and CTβ-488(green) into left and right eyes of WT and C1q KO mice. C1q KO mice at P10 (Ab) and P30 (Ad) have significant intermingling (yellow, overlap) between RGC axons from left and right eyes compared to littermate WT controls (Aa and Ac). Scale bar, 200 μm.

(B and C) Quantification of the percentage of dLGN-receiving overlapping inputs in C1q KO versus WT controls at P10 (B) and P30 (C). C1q KO mice exhibit significantly more overlap than WT mice, regardless of threshold. Data are represented as mean ± SEM (P10, n = 8 mice, $p < 0.01$ [t test] at 5% threshold and $p < 0.05$ at 30% threshold; P30, n = 6 mice, $p < 0.009$ at 5% threshold, and $p < 0.01$ at 30% threshold).

techniques to investigate the refinement and elimination of retinogeniculate synapses in the dLGN of mice that lack the A chain of C1q (C1q KO). These mice cannot assemble or secrete a functional C1q protein and thus are unable to activate the classical complement cascade (Botto et al., 1998).

To visualize the pattern of retinogeniculate projections, we first performed anterograde tracing of RGC afferents by injecting the β subunit of cholera toxin conjugated to Alexa 594 dye (CTβ-594) or to CTβ-Alexa 488 into the left and right eyes, respectively, of wild-type (WT) and C1q KO mice at several postnatal ages (P5, P10, and P30). In the mouse LGN, the majority of axons from the ipsilateral eye (uncrossed projections) have segregated into an eye-specific patch in the dorsomedial region of the dLGN by P10 (Figure 4Aa). The pattern of RGC inputs to the dLGN appeared normal in C1q KO mice at P5, a time point before significant segregation occurs. In contrast, at P10, the amount of dLGN territory occupied by contralateral (crossed) retinal projections was notably larger, and in many cases, the ipsilateral projections appeared more diffuse in C1q KOs compared to age-matched WT mice and littermate controls (Figure 4Aa versus Figure 4Ab). Consistent with these observations, the

dLGNs in C1q KOs have significant defects in eye-specific segregation. We observed significant overlap between contralateral and ipsilateral RGC projections in the dLGN of C1q KOs, which resulted in a larger overlap zone (Figure 4Aa versus Figure 4Ab, bottom row).

We quantified these data using an established multithreshold method of analysis (Torborg and Feller, 2004; Bjartmar et al., 2006) and found that the dLGNs of P10 C1q KO mice had a significantly higher percentage of overlapping projections, independent of threshold (Figure 4B). The lack of a phenotype at P5 suggests that refinement defects in the P10 C1q KO mice are not due to early defects in axonal path finding or targeting. In addition, this segregation phenotype can not be explained by differences in the number of RGCs projecting axons to the dLGN in C1q KO mice, as there was no difference in the number of cells in the peripheral or central regions of whole-mount retinas between C1q KO and controls (Figure S2A).

To find out whether the dLGN refinement defect in C1q KO mice was transient or sustained, we next examined mice at P30, several weeks after segregation is normally completed. Surprisingly, this eye-specific segregation phenotype was still evident in P30 C1q KOs (Figure 4Ac versus Figure 4Ad, bottom row). Normally, by P30, there is very little overlap between the two eyes, but C1q KOs still had significant overlapping retinal projections (Figures 4A and 4C). The segregation defects at P30 were thus sustained and similar to those observed at P10, suggesting that many dLGN neurons remain binocularly innervated into adulthood.

The segregation defects we measured in C1q KOs were not due to effects of abnormal retinal activity. Multielectrode recordings of RGC firing patterns indicated that C1q KO retinas (P5) produced spontaneous correlated waves of activity that were indistinguishable from age-matched controls (Figure S2B). Thus, C1q KOs exhibit significant and sustained defects in retinogeniculate synaptic refinement that cannot be attributed to a change in RGC number or early patterned activity.

LGN Neurons Remain Multiply Innervated in C1q KO Mice

If C1q is required for synapse elimination, then an increase in synapse number would be expected in its absence. Indeed, we observed a general increase in the intensity of synaptic staining in the dLGN of C1q KO mice compared to littermate controls (Figure S3). Despite these differences in synaptic staining, the overall morphology of LGN neurons was similar in C1qKO and WT mice (Figure S4E). We next used electrophysiology to directly measure whether the number of functional retinogeniculate synapses are increased in the dLGNs of C1q KOs. We performed patch-clamp recordings from acute brain slices of P30 mice and measured the amplitude of responses evoked in relay cells by stimulating RGC axons in the optic tract (Figure 5A). Small incremental increases in stimulus intensity were used in order to recruit individual RGC axons in a graded manner, thus giving an indication of the number of axons that innervate each cell (Hooks and Chen, 2006).

As an initial analysis, we first classified the cells based on their overall response properties using the criteria defined by Hooks and Chen (2006). Cells with one or two large distinct inputs were classified as refined, those with greater than two inputs that were less defined were classified as resolving, and cells with numerous small indistinct inputs were classified as nonrefined. Representative recordings obtained from dLGN neurons from a WT and a C1q KO mouse are shown in Figure 5B. As previously reported, we found that by P30 the majority of WT cells were innervated by only one or two axons and thus were in the refined category. We found, however, that 81% of C1q KO neurons were multiply innervated and thus still classified as resolving, indicating a deficit in synapse elimination (Figure 5C, C1q KO $n = 21$, WT $n = 30$ cells, $p < 0.001$). No cells were in the nonrefined category, showing that some synapse elimination and maturation had occurred even in the absence of C1q. We next determined the number of axons that innervated each relay neuron. Inputs were counted when there were distinct steps between the responses; this analysis is likely to underestimate the real input number but allows a comparison to be made between the two conditions. We found that the majority of WT cells received one or two inputs, whereas the majority of C1q KO cells were innervated by four or more inputs (Figure S4A, C1q KO $= 4 \pm 0.3$ inputs, WT $= 2.2 \pm 0.2$ inputs, $p < 0.001$). When the individual inputs are plotted out, there is a clear rightward shift in the distribution of the inputs in the C1q KO, with some LGN neurons having as many as seven inputs (Figure 5D).

Interestingly, the average amplitude of evoked responses was significantly reduced in C1q KOs (Figure S4D). We observed many more small amplitude responses in C1q KOs than in WTs, as shown by a cumulative probability plot of individual AMPA response amplitudes (Figure 5E). These smaller inputs correlate with the innervation pattern seen at early stages of development. The maximum input amplitude observed in C1q KO neurons is similar to WT, however, demonstrating that despite the multiple innervation of the LGN neurons in the C1q KO mice, there has been functional maturation and strengthening of at least one axonal input (Figure S4C). In summary, these experiments show that the anatomical retinogeniculate refinement defects observed in the C1q KO mice are accompanied by a corresponding defect in the elimination of functional synaptic inputs.

Role of the Complement Cascade in Developmental Synapse Elimination

C1q might mediate synapse elimination by its known role as the initiating protein of the classical complement cascade or alternatively by a novel mechanism. To address whether C1q acts via the classical complement cascade, we next investigated whether the pivotal protein of the complement cascade, C3, is present in the developing

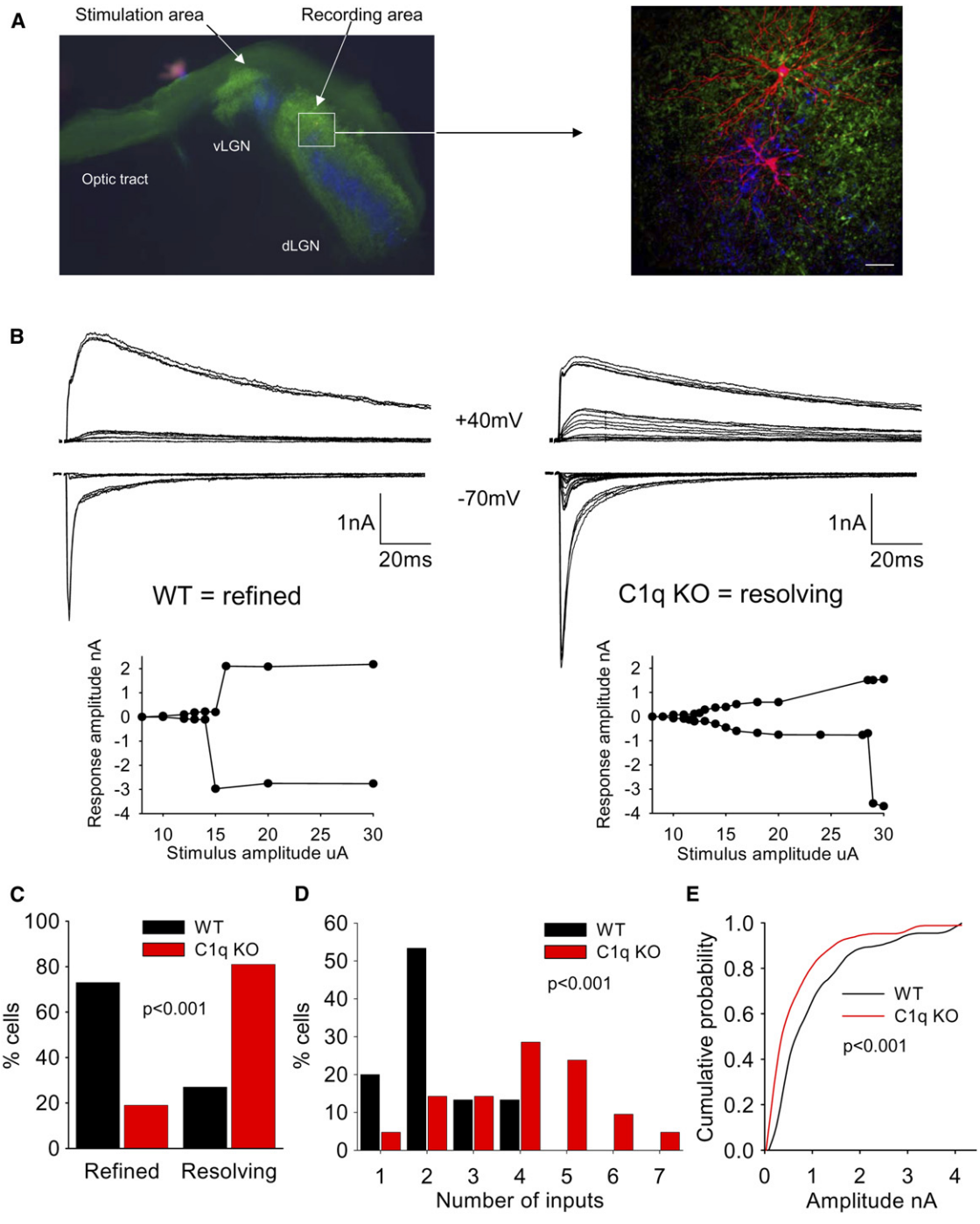

Figure 5. LGN Neurons Remain Multiply Innervated in C1q-Deficient Mice

(A) (Left) Representative image showing the LGN slice recording preparation as described (Supplemental Data). Parasagittal brain slices were prepared from ~P30 mice), and CTβ was used to label contralateral retinal projections in green and ipsilateral projections in blue 24 hr before slices were made. (Right) Electrophysiological recordings were made from LGN relay neurons (in red) in the proximal third of the dorsal LGN (contralateral region), and the optic tract was stimulated in the region next to the ventral LGN. The right panel is a zoomed confocal projection showing dye-filled neurons. Scale bar, 40 μm.

(B) Representative raw data traces of individual LGN neurons recorded from a WT and C1q KO mouse. (Top) Overlay of individual stimulus trials at all stimulus intensities to show individual responses. The stimulus artifact has been removed for clarity. Currents at −70 mV are mediated predominantly by activation of AMPA receptors, and those at +40 mV are due to NMDA receptor activation. (Bottom) Plot of stimulus intensity against response amplitude for the cells shown.

brain and necessary for synapse elimination. We immunostained cryosections of postnatal rodent brain using C3-specific antisera. Punctate C3 immunoreactivity was present in the postnatal rodent dLGN and cortex, but C3 levels were significantly lower in these regions in mature animals (Figure 6A, Figure S5), which is consistent with published reports (Cowell et al., 2003). In addition, confocal imaging of double immunofluorescence labeling of postnatal dLGN sections revealed that several C3-positive puncta colocalized or were closely apposed to synaptic puncta (Figure S5B).

The developmental expression and localization of C3 in the developing LGN is similar to that of C1q, suggesting that the classical complement cascade is involved in synapse elimination. To directly investigate this, we examined mice deficient in C3 to determine whether absence of C3 mimics the phenotype we observed in the LGNs of C1q KOs. We repeated the anterograde tracing experiments and electrophysiological recordings of retinogeniculate synapses in C3 KO mice and age-matched controls. Consistent with our hypothesis, C3 KOs displayed defects in eye-specific segregation and synapse elimination that closely mimic the C1q KO phenotype. C3 KO mice had significant defects in eye-specific segregation, both at P10 and P30 (Figures 6B–6D). Quantification of the percentage of dLGN occupied by overlapping retinal axons from both eyes indicates that C3 KO mice, much like C1q KOs, had significantly more overlapping projections than age-matched and littermate controls. No obvious defects in synapse elimination were observed at the neuromuscular junction in C3 KO mice (Figure S6). Electrophysiological recordings of P30 dLGN neurons indicate that LGN neurons recorded from C3 KO mice had similar response properties to C1q KO mice (Figure 6E). The majority of C3 KO cells were classified as resolving (77%) rather than refined (23%), compared to WT cells, which are mostly refined by this age (Figure 6E, C3 KO n = 13, WT n = 30, $p = 0.006$). The remarkably similar phenotypes in the C1q and C3 KO mice, along with the presence of C3 cleavage and activation in the developing but not adult rodent brain (Cowell et al., 2003), provide evidence that activation of the classical complement cascade occurs during normal postnatal CNS development and helps to mediate normal developmental synapse elimination.

C1q Is Localized to Adult Retinal Synapses at Early Stages of Glaucoma

Growing evidence suggests that one of the earliest events in neurodegenerative diseases is substantial synapse loss (Selkoe, 2002). Glaucomas are characterized by the death of RGCs and are often associated with elevated intraocular pressure (IOP) (Ritch et al., 1996). Our recent microarray study discovered that C1q and other complement genes are among the first upregulated in DBA/2J glaucoma (G.R.H. and S.W.M.J., unpublished data). Given our findings that C1q mediates developmental synapse elimination, we investigated whether C1q is re-expressed and localized to synapses at early stages of glaucoma using DBA/2J mice (see Libby et al., 2005).

We looked at the timing and localization of C1q in the RGCs and IPL of retinas of glaucomatous DBA/2J and control mice. The control mice were from the DBA/2J-*Gpnmb*$^{+}$ substrain that is genetically matched to the DBA/2J strain but does not develop elevated IOP with age. Significant RGC loss and nerve damage is absent in almost all control mice but does occur at low frequency (Howell et al., 2007). Synaptic C1q was not observed in the IPL of four young DBA/2J mice (2.2 months) or in the retinas of five aged control mice (10.5 months) (Figure 7Ab). Punctate staining was observed in one aged control eye (10.5 months). This may reflect the low incidence of age-related RGC loss and nerve damage in this strain (Howell et al., 2007). In marked contrast to the young DBA/2J and control mice, punctate C1q immunoreactivity was present in the IPL of 11 out of 15 retinas from aged DBA/2J mice (four of four at 6 months and seven of 11 at 10.5 months) (Figure 7Aa). This punctate C1q staining was present in five eyes that were determined to have the "no or early" stage of glaucoma by optic nerve assessment and have no detectable RGC loss (see the Supplemental Data). Confocal imaging revealed that many C1q-positive puncta colocalized with synaptic puncta in the IPL of retinas from DBA/2J mice, and this synaptic localization of C1q was similar to our findings in the IPL of postnatal retinas (Figure 7Bg). In addition, we observed a more pronounced increase in C1q punctate staining in the IPL of retinas from eyes with moderate glaucoma (Figures 7Bb and 7Bh). In moderate glaucoma, there is some RGC and synapse loss, as indicated by axonal damage in the optic nerve and a patchy loss of PSD-95 staining in the IPL (Figures 7Bd and 7Bf). C1q punctate staining was also observed at lower levels in retinas of DBA/2J mice with severe glaucoma and corresponded to a further decrease in the density of PSD-95 positive puncta, reflecting the substantial loss of RGCs at this late stage of the disease (data not shown).

In order to further investigate C1q expression in this mouse model of glaucoma, we performed quantitative real-time PCR on retinal RNA from 10.5-month-old

(C) Categorization of the response properties of LGN relay neurons. Refined cells receive one or two distinct inputs and resolving cells receive three or more inputs. The majority of C1q KO neurons are still in the resolving category, whereas most WT neurons are in the refined category (C1q KO n = 21, WT n = 30 cells, $p < 0.001$).

(D) Plot of individual axonal input numbers for WT and C1q KO neurons. C1q KOs remain multiply innervated (average of 4 ± 0.3 inputs, n = 21) compared to WT controls (average of 2.2 ± 0.2 inputs, n = 30, $p < 0.001$).

(E) Individual AMPA receptor inputs plotted in a cumulative probability histogram. The average AMPA input amplitude is decreased in the C1q KO (0.6 ± 0.1 nA, n = 84) compared to WT (1 ± 0.1 nA, n = 66, $p < 0.001$).

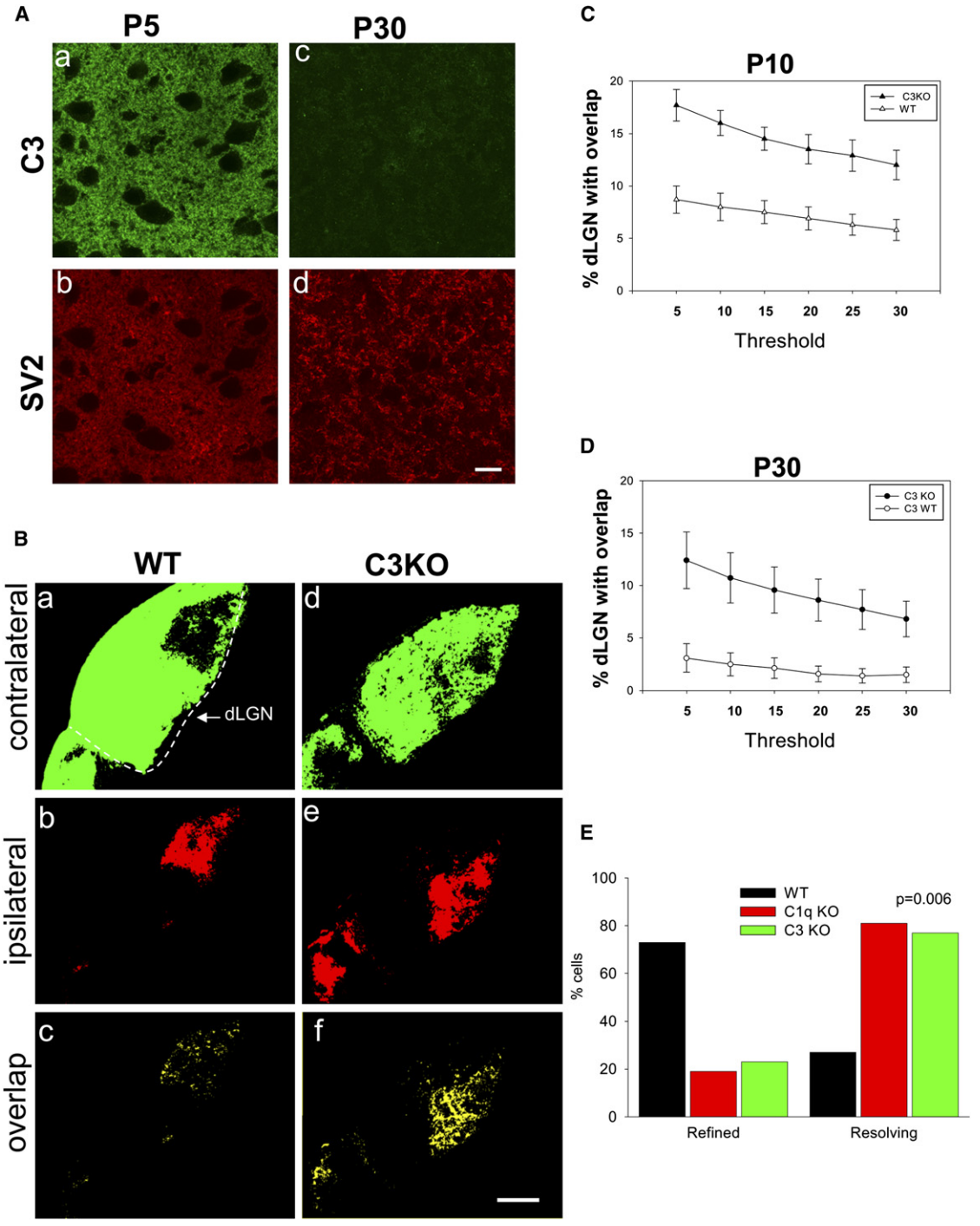

Figure 6. Mice Deficient in C3 Also Have Defects in Synapse Elimination

(A) Double staining of C3 (green) with the presynaptic antibody, SV2 (red) revealed robust C3 staining in the developing (P5), but not the mature dLGN ([Aa] and [Ab] versus [Ac] and [Ad]). Scale bar, 10 μm. C3 immunoreactivity was specific for C3, as C3 antibodies failed to stain brain sections prepared from C3 KO mice (Figure S5).

(B) Anterograde tracing experiments show that C3 KO mice at P30 exhibit significant overlap (yellow) between RGC axons from left and right eyes compared to littermate WT controls.

(C and D) Quantification of the percentage of dLGN-receiving overlapping inputs in C3 KO versus WT controls at P10 (C) and P30 (D). C3 KO mice exhibit significantly more overlap than littermate control mice, regardless of threshold. Data are represented as mean ± SEM (P10, n = 8 mice, $p < 0.02$ [t test] at 5% threshold and $p < 0.05$ at 30% threshold; P30, n = 9 mice, $p < 0.02$ at 5% threshold, and $p < 0.03$ at 30% threshold).

DBA/2J mice with different stages of disease, as well as age-matched DBA/2J-*Gpnmb*$^{+}$ controls. Compared to controls, *C1qA* and *C1qB* RNA levels were elevated in five out of ten retinas with no or early glaucoma, and increased up to 25-fold in eyes with moderate glaucoma (Figure 7C). The timing and degree of C1q gene expression corresponded to the synaptic pattern of C1q protein in the IPL of retinas with early and moderate glaucoma. Together, these findings indicate that C1q is expressed at early stages of glaucoma and becomes relocalized to synapses in the adult IPL before significant synapse loss and RGC death. This suggests that reactivation of complement-mediated synapse loss occurs as a crucial early event in glaucoma.

DISCUSSION

The Classical Complement Cascade Mediates Developmental CNS Synapse Elimination

Our finding that the classical complement cascade helps to mediate developmental CNS synapse elimination adds to the growing evidence that components of the immune system contribute to brain development and function (Boulanger and Shatz, 2004). Indeed, many components of the complement cascade have been reported to be present in the normal developing brain (Morgan and Gasque, 1996; Johnson et al., 1994), and it has long been suggested that they may play some normal role during brain development. Unlike most nonneuronal cell types, which express high levels of transmembrane complement inhibitors, developing CNS neurons are able to bind complement C1q and spontaneously activate the classical complement cascade independently of antibodies (Singhrao et al., 2000). The classical complement cascade is part of the innate immune system, but recent studies have found that components of the adaptive immune system also participate in developmental synaptic refinement. In particular, class I major histocompatibity complex (MHC1) molecules are expressed by neurons and required for normal retinogeniculate refinement (Huh et al., 2000), raising the question of whether there are relevant interactions between complement and MHC I proteins.

As C1q is a secreted soluble protein, a crucial question raised by our findings is the identity of its synaptic receptor. Neuronal pentraxins (NP1 and NP2/NARP) are secreted synaptic proteins with 20%–30% homology to the immune pentraxins, pentraxin-3 (PTX3) and C-reactive protein (CRP). PTX3 and CRP are capable of opsonizing and marking cells for phagocytosis and are well known binding partners of C1q (Nauta et al., 2003). Interestingly, NP1 and NP2 directly bind C1q (M. Perin, personal communication), raising the possibility that C1q and NPs could interact at early stages of retinogeniculate refinement. Both C1q and NP1/2 KO mice have similar defects in retinogeniculate eye-specific segregation at early stages (P10), but in contrast to the C1q KOs, these defects are transient in NP KO mice (Bjartmar et al., 2006). Similarly, cerebellins are secreted C1q-like molecules that are highly synaptically localized and participate in CNS synaptic plasticity (Hirai et al., 2005). The only known synaptically accumulated protein that is membrane anchored and also binds to C1q is the prion protein Prpc. Prpc is a particularly intriguing candidate, given that in its abnormal conformation it strongly activates C1q activity (Mitchell et al., 2007).

How Does the Complement Cascade Eliminate CNS Synapses?

Our findings demonstrate that C1q is localized to many developing synapses and that the classical complement cascade is necessary for synapse elimination. What determines which synapses will be eliminated by complement, and which will be maintained? The retinogeniculate synapse elimination phenotypes that we have observed in the C1q and C3 KO mice resemble the phenotypes that have been observed when electrical activity of developing RGCs is blocked (Huberman, 2007). Electrical activity is necessary to drive synapse elimination both in the developing CNS and at the NMJ. An intriguing model was proposed over a decade ago for how activity may drive synapse elimination. This model proposes that strong synapses, which are effective in driving postsynaptic responses, actively punish and eliminate nearby weaker synapses by inducing two postsynaptic signals: a short-range "protective" signal and a longer-range elimination or "punishment" signal (Jennings, 1994). A similar activity-based competition process is necessary to eliminate terminal branches of retinal axons (Hua and Smith, 2004). Our findings raise the intriguing possibility that a similar mechanism drives synapse elimination at retinogeniculate synapses and that the activity-dependent punishment signal is an activator or component of the complement cascade. A well-known feature of the complement cascade is that the highly reactive C3b fragment has only short diffusion ability before it becomes inactive so that little innocent bystander damage can occur. The protective signal might be one of the known complement inhibitors. We do not know yet whether C1q initially tags most synapses and its activation leads to elimination of weak synapses or whether only weak synapses can bind C1q. Thus, important future questions are whether inhibition of electrical activity blocks the normal complement cascade activation within the developing brain and, if so, how to understand the molecular mechanism by which activity activates the cascade.

How are complement-tagged synapses eliminated? Since both C1q and C3 are required for normal synapse

(E) Electrophysiological recordings of ~P30 dLGN neurons indicate that the majority of neurons in C3 KO mice remain in the resolving category, similar to C1q KO mice, and in contrast to WT neurons which are mostly refined (C3 KO, n = 13; C1q KO, n = 21; WT, n = 30 cells; p = 0.006).

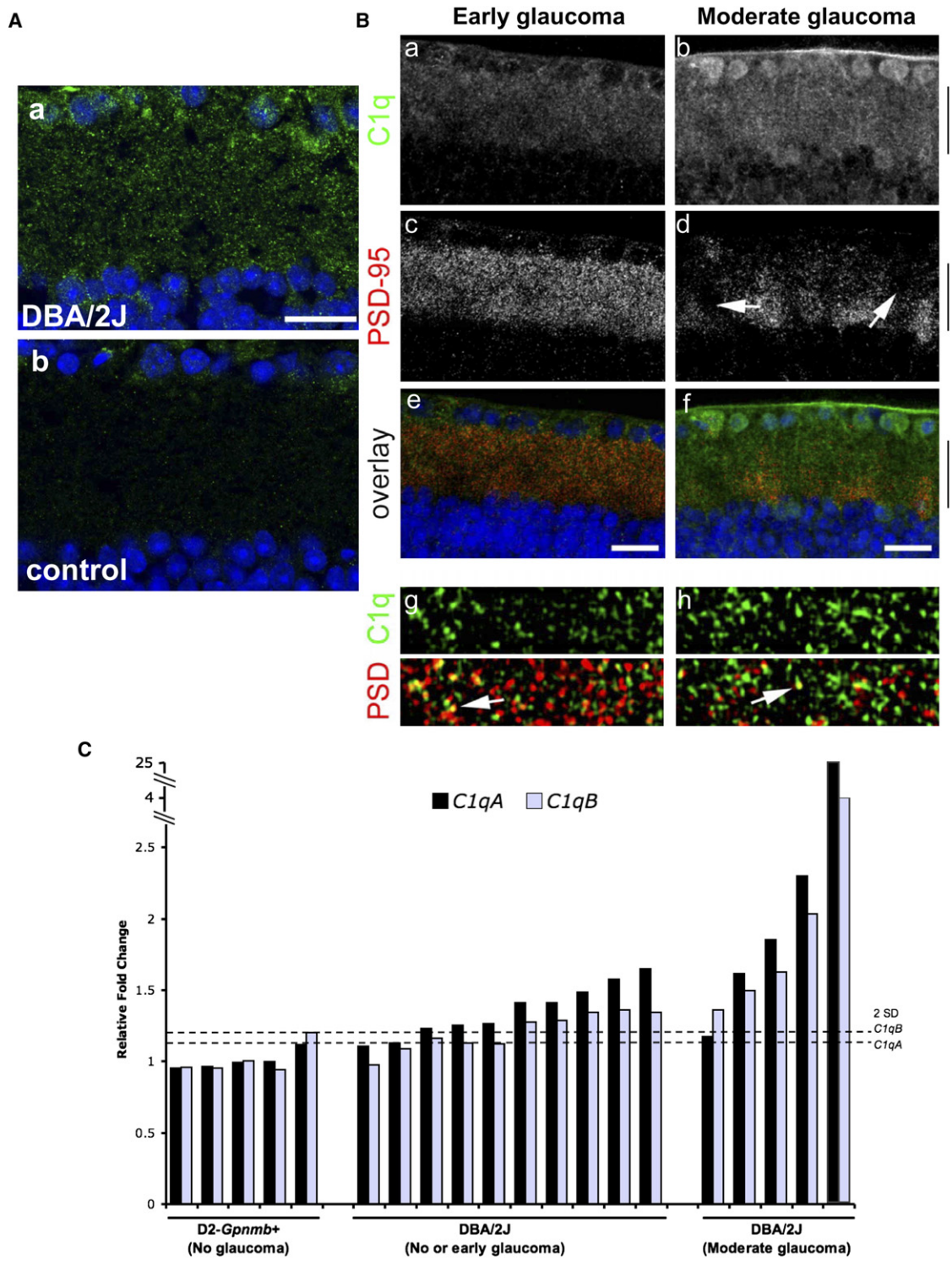

Figure 7. C1q Is Localized to Synapses in Glaucoma and Is an Early Indicator of Disease

(A) (Aa) Punctate C1q staining (green) was observed in the IPL of retinas classified as having no or early glaucoma. (Ab) In contrast, this pattern of C1q staining was not observed in the majority of retinas from the control DBA/2J-*Gpnmb*$^{+}$ strain (10.5 months of age). Scale bar, 10 uM.

(B) Stacked confocal images of C1q and PSD95 staining in the synaptic inner plexiform layer (IPL) of retinas from DBA/2J mice. (Ba–Bf) Representative sections from an eye with early glaucoma (left panels) and moderate glaucoma (right panels) stained with the indicated antibodies C1q (green), PSD-95 (red), and DAPI (blue). In the section from an eye with early glaucoma, there is punctate C1q staining before obvious RGC (DAPI) or synapse

elimination and are both localized to developing synapses, synapses to be eliminated most likely need to be tagged by activated C3 (C3b). Further downstream activation of the membrane attack complex is unlikely in the normal brain, because neurons express high levels of the downstream complement inhibitor CD59 (Wang et al., 2007). It is likely that the C3b-opsonized synapses are phagocytosed by resident microglia, the primary phagocytic cells in the brain and the only known CNS cells to express the C3 receptor (Gasque et al., 1998). Binding of C3b to this receptor is well established to induce phagocytosis. Activated microglia secrete most complement cascade components, including particularly high amounts of C1q, and are localized in the gray matter of cerebellum, hippocampus, and other brain regions during a narrow window of postnatal development that coincides with the peak of synapse formation and elimination (Dalmau et al., 1998; Maslinska et al., 1998; Fiske and Brunjes, 2000; our unpublished data), and it has been speculated that activated microglia could participate in synaptic remodeling. Microglia are also activated and recruited to motor neuron synapses after axotomy in a process known as "synaptic stripping," in which microglia rapidly displace or engulf synapses (Schiefer et al., 1999). There are already good precedents that part of a cell can be phagocytozed in isolation—for example, in axon pruning and photoreceptor outer segment shedding.

The Complement Cascade Mediates Only a Portion of Synapse Elimination

Our findings provide evidence for both complement-dependent and -independent mechanisms of synapse elimination. In the PNS, synapse elimination at the NMJ is carried out by perisynaptic Schwann cells (SCs), which engulf and eliminate presynaptic terminals by a process known as "axosome" shedding (Bishop et al., 2004). This process is not likely mediated by the complement cascade, as we did not observe a synapse elimination phenotype at the NMJ in complement KO mice (Figure S6). This is not surprising, as SCs do not express known complement receptors. Thus, complement-dependent synapse elimination may specifically occur within the CNS.

Even in the CNS, although our studies provide anatomical and electrophysiological evidence that C1q and C3 KOs have significant defects in eye-specific segregation and synapse elimination, these mice still undergo some degree of synaptic refinement and synaptic pruning, indicating that complement-independent synapse elimination also occurs. We found that C1q and C3 protein levels and synaptic localization were highest between P4 and P10 and were necessary for eye-specific segregation, although it remains possible that complement could play an additional role in later stages of development (Mastellos and Lambris, 2002). Indeed, recent evidence indicates that activity-dependent synaptic remodeling occurs in the dLGN at several developmental stages (Hooks and Chen, 2006). Eye-specific segregation and synapse refinement occurs largely before P10, but then later, fine-scale pruning occurs in binocular zones as well as in the monocular regions as described here and in previous studies (Jaubert-Miazza et al., 2005; Hooks and Chen, 2006). Initially, dLGN neurons have a large number of afferents (up to ten) with small synaptic strength, but by P30, each dLGN neuron normally receives strong, stable inputs from only one to two RGC axons. We found that the majority of C1q and C3 KO cells were innervated by four or more inputs at P30, with some LGN neurons having as many as seven inputs. While complement-deficient mice generally had many smaller amplitude inputs, one of their synapses typically was functionally strengthened to become a larger input, indicating that C1q normally functions to eliminate these weaker, inappropriate synapses during development, while C1q-independent mechanisms strengthen appropriate synapses.

Role of Glia in Complement-Mediated Synapse Elimination in Development and Disease

In the developing brain, astrocytes are generated neonatally and persist in an immature phenotype until about P14, prior to undergoing phenotypic maturation. Our findings suggest that a signal produced by immature astrocytes in the normal developing brain and retina acts as a switch that times expression of complement protein C1q, thus enabling a developmental window for complement-dependent synapse elimination. The appearance of astrocytes, and the localization of C1q (and C3) at synapses in the postnatal brain and retina, coincides with this critical period of synaptic pruning. Immature astrocytes may create a permissive window of time during which activity-dependent instructive signaling can control which synapses are retained or eliminated. Consistent with this possibility, Muller and Best (1989) found that immature astrocytes transplanted into the primary visual cortex of adult cats were able to restore ocular dominance plasticity. Interestingly, C1q was one of the few genes expressed selectively during the critical period for visual cortex development in kitten (Prasad and Cynader, 1994), and polymorphisms in C3 were found to be the strongest genetic marker associated with excellent memory task ability in a quantitative trait loci (QTL) analysis of heritable traits associated with memory performance (Nilsson et al., 1996). The identification of the soluble

loss (PSD-95). In a section with no RGC loss (DAPI) from an eye with moderate glaucoma, punctate C1q staining is more intense and there is focal synapse loss (PSD-95, arrows). (Bg and Bh) Merged images of C1q (green), PSD-95 (red), and DAPI (blue) show that C1q is localized to synapses in early and moderate stages of glaucoma. Scale bar, 20 μm.

(C) *C1qA* and *C1qB* RNA levels are elevated early in glaucoma. *C1qA* (black bars) and *C1qB* (purple bars). Increases in *C1q* expression occurred in five out of ten retinas with no or early glaucoma and five out of five retinas with moderate glaucoma (expression levels relative to average DBA/2J-*Gpnmb*$^{+}$ controls, >2 SD considered elevated).

astrocyte-derived signal that triggers C1q upregulation in neurons will be an important next step to investigate the specific mechanisms by which astrocytes and complement control synapse elimination in vivo.

Lastly, our findings have important implications for understanding the mechanism of synapse loss in neurodegenerative disease. Our findings strongly suggest that the normal developmental mechanism of complement-mediated synapse elimination that we have described here becomes aberrantly reactivated in the adult CNS after injury or neurodegenerative disease. After CNS neurological injury or disease, C1q is rapidly upregulated within microglia and neurons concurrently with the appearance of reactive astrocytes. For instance, C1q is profoundly upregulated in human Alzheimer's disease (AD), glaucoma, and ALS (Fonseca et al., 2004; Dangond et al., 2004; Stasi et al., 2006; Steele et al., 2006). As reactive astrocytes are prominent in these conditions and antigenically resemble immature astrocytes, we hypothesize that, in early stages of neurodegenerative disease, reactive astrocytes re-express the signal that induces C1q expression in developing neurons, thus playing an early role in a pathophysiological process that ultimately leads to synapse loss and then neuronal death.

The DBA/2J inherited mouse model promises to be a useful tool to investigate this possibility further. Our study demonstrates that C1q protein is localized to retinal synapses in these mice and that this occurs early in the disease before and/or concurrent with synapse loss. Although further studies are needed to determine the exact relationship of these findings to RGC demise, substantial synapse loss and neuron death appears to follow synaptic C1q relocalization, as some eyes had synaptically relocalized C1q prior to RGC loss and optic nerve damage. These findings suggest that, just as in development, C1q in the adult glaucomatous retinas tags synapses for elimination even at early stages of disease. This early complement-dependent synapse loss could drive the dendritic atrophy and axon degeneration that occur with progression of the disease. In future studies, it will be possible to directly test the role of C1q and C3 in mediating neurodegeneration by backcrossing their mutant genes into the DBA/2J background (see John et al., 1999) or by the use of pharmacological inhibitors of the complement pathway (Sahu and Lambris, 2000; Barnum, 2002). If so, pharmacological inhibition of the classical complement cascade may inhibit synapse loss and neurodegeneration not only in glaucoma but in many other neurodegenerative diseases including ALS, AD, and multiple sclerosis.

EXPERIMENTAL PROCEDURES

Materials and other experimental procedures are described in the Supplemental Data.

Neuron and Astrocyte Cultures

Step-by-step protocols for all procedures are available on request to barres@stanford.edu. RGCs were purified by sequential immunopanning to greater than 99.5% purity from P5 Sprague-Dawley rats and cultured in serum-free media as described (Meyer-Franke et al., 1995; Supplemental Data). Cortical astrocytes were prepared from P1-P2 rat cortices as previously described (Ullian et al., 2001; Supplemental Data).

RGC Gene Expression Analysis Using Affymetrix GeneChip Arrays

Purified RGCs were plated at a density of ~100,000 cells per well in 6-well dishes and cultured in the presence or absence of an astrocyte feeding layer for 4 days. Total RNA was harvested using RNeasy Mini Kit (QIAGEN). cDNA was synthesized from 2 μg total RNA using the GIBCO-BRL Superscript Choice system and a T7-$(dT)_{24}$ primer as described (Wang et al., 2007). Primer sequence and details on hybridization to Affymetrix Gene Array are described in the Supplemental Data.

Semiquantitative RT-PCR

Total RNA was prepared as above from RGCs cultured alone or with an astrocyte feeding layer. RNA (1 μg total) was reverse transcribed using RETROScript (Ambion) and one twentieth of resulting cDNA product was used for PCR. Results shown are representative of three biological replicates. PCR conditions are described in the Supplemental Data.

In Situ Hybridization

In situ hybridization was performed on 12 μm fresh frozen PBS perfused retinal sections as previously described (Schaeren-Wiemers and Gerfin-Moser, 1993) using probes generated with the DIG RNA labeling kit (Roche Applied Science) as per the manufacturer's instructions (see the Supplemental Data).

Mice

C1qAKO mice (C57BL6 background) were generously provided by M. Botto (Botto et al., 1998). C3KO mice (and a control strain) were obtained from The Jackson Laboratory. DBA/2J (D2) mice and a control substrain (full name DBA/2J-*Gpnmb*$^{+}$/Sj) were from our colony (Sj) maintained at The Jackson Laboratory, and glaucoma in our colony has been studied extensively (Libby et al., 2005). Details on mouse strains are described in the Supplemental Data.

Immunocytochemistry

Brains and eyes were immersed in 4% paraformaldehyde (PFA), fixed overnight at 4°C, and cryoprotected in 30% sucrose. For complement and synaptic staining, tissue was perfused with PBS before fixation, embedded in a 2:1 mixture of OCT:20% sucrose PBS, and cryosectioned (10–15 microns). Sections were dried, washed three times in PBS, and blocked with 2% BSA+ 0.2% Triton X in PBS for 1 hr. Primary antibodies were diluted in antibody buffer (+ 0.05% triton + 0.5% BSA) as follows: C1q (Quidel goat anti human C1q, 1:1000), C3 (Cappel goat anti-Rat, 1:1000 or Rabbit anti-C3c, 1:1000 [provided by J.D.L.]), SV2 (Developmental Studies Hybridoma Bank, 1:50), and PSD95 (Zymed, rabbit, 1:200) and incubated overnight at 4°C. Secondary Alexa-conjugated antibodies (Invitrogen) were added at (1:200–1:500 in Ab buffer) for 2 hr at room temperature. Slides mounted in Vectashield (+DAPI) were imaged using a CCD camera (SPOT) or a Leica SP2 AOBS confocal laser scanning microscope.

Array Tomography

Two mice, postnatal day 7, were perfused intracardially with PBS followed by 4% PFA in PBS. The tissue was then processed for array tomography as described in Micheva and Smith (2007) and in the Supplemental Data.

Labeling of Retinogeniculate Afferents

Mouse pups were anesthetized with inhalant isofluorane. Mice received intravitreal injections of cholera toxin-β subunit (CTβ) conjugated to Alexa 488 (green label) in the left eye and CTβ conjugated

to Alexa 594 (red label) into the right eye as described in Bjartmar et al. (2006) and in the Supplemental Data.

Quantification of LGN Images and Preparation of Photomicrographs

Images were digitally acquired with a color CCD camera (SPOT). All images were collected and quantified "blind," and age-matched littermate controls were used in addition to age-matched standard C57BL6 mice. Gains and exposures were established for each label. Raw images of the dLGN were imported to Photoshop (Adobe),and the degree of left and right eye axon overlap in dLGN was quantified using the multithreshold protocol as previously described (Bjartmar et al., 2006; Supplemental Data).

Electrophysiological Recordings

Mice aged P26–P34 were euthanized, and parasagittal brain slices containing the LGN (250 μm) were cut on a vibratome and whole-cell voltage-clamp recordings of thalamic relay neurons from the contralateral region of the dLGN performed following the method of Hooks and Chen (2006) (see the Supplemental Data). For statistical analysis, a t test was used to compare two groups of data. Values are expressed as mean ± SEM.

Determining Stage of Glaucoma

Glaucoma was assessed using standard procedures as previously described (Libby et al., 2005; Howell et al., 2007). Briefly, retrobulbar portions of the optic nerves were fixed, processed, embedded in plastic, and sectioned. Sections were stained with paraphenylenediamine (PPD), which stains all myelin sheaths but differentially stains the axoplasm of sick or dying axons darkly. The damage level of each nerve (no or early, moderate and severe) was determined using the consensus of three masked investigators (see the Supplemental Data).

C1q Real-Time PCR

C1qA and *C1qB* RNA expression levels were assessed in 15 eyes from 10.5-month-old DBA/2J mice (ten no or early and five moderate glaucoma), and five DBA/2J-*Gpnmb*$^{+}$ "control" eyes. The retinas were dissected free and placed in RNAlater (QIAGEN) for at least 24 hr, and RNA was isolated using Microkit RNA extraction (QIAGEN). For each eye, 500 ng of RNA was used to generate first-strand cDNA using Message Sensor RT (Ambion). Expression levels were assessed for *C1qA*, *C1qB* as well as the three normalizers. Real-time PCR reactions were prepared using Power SYBR Green PCR (Applied Biosystems) and run on the 7900HT Fast Real-Time PCR System (Applied Biosystems). Details on the PCR conditions, primer sequences, and relative expression values are described in the Supplemental Data.

Supplemental Data

Supplemental Data include Supplemental Experimental Procedures, six figures, and Supplemental References and can be found with this article online at http://www.cell.com/cgi/content/full/131/6/1164/DC1/.

ACKNOWLEDGMENTS

We thank Arnon Rosenthal, Alex Goddard, David Stellwagen, Axel Nimmerjahn, Alissa Winzeler, and David Feldheim for helpful comments on the manuscript. This work was generously supported by grants from the National Institute on Drug Abuse (DA15043; B.A.B.), a Larry H. Hillblom Fellowship (B.S.), a Human Frontier Fellowship (N.J.A.), and a Helen Hay Whitney Fellowship (A.D.H.). S.W.M.J. is an Investigator of the Howard Hughes Medical Institute. We would like to extend special thanks to Jonathan Pollack for his support and encouragement of this work.

Received: January 19, 2007
Revised: August 15, 2007
Accepted: October 15, 2007
Published: December 13, 2007

REFERENCES

Barnum, S.R. (2002). Complement in central nervous system inflammation. Immunol. Res. *26*, 7–13.

Bishop, D.L., Misgeld, T., Walsh, M.K., Gan, W.B., and Lichtman, J.W. (2004). Axon branch removal at developing synapses by axosome shedding. Neuron *44*, 651–661.

Bjartmar, L., Huberman, A.D., Ullian, E.M., Renteria, R.C., Liu, X., Xu, W., Prezioso, J., Susman, M.W., Stellwagen, D., Stokes, C.C., et al. (2006). Neuronal pentraxins mediate synaptic refinement in the developing visual system. J. Neurosci. *26*, 6269–6281.

Botto, M., Dell'Agnola, C., Bygrave, A.E., Thompson, E.M., Cook, H.T., Petry, F., Loos, M., Pandolfi, P.P., and Walport, M.J. (1998). Homozygous C1q deficiency causes glomerulonephritis associated with multiple apoptotic bodies. Nat. Genet. *19*, 56–59.

Boulanger, L.M., and Shatz, C.J. (2004). Immune signalling in neural development, synaptic plasticity and disease. Nat. Rev. Neurosci. *5*, 521–531.

Christopherson, K.S., Ullian, E.M., Stokes, C.C., Mullowney, C.E., Hell, J.W., Agah, A., Lawler, J., Mosher, D.F., Bornstein, P., and Barres, B.A. (2005). Thrombospondins are astrocyte-secreted proteins that promote CNS synaptogenesis. Cell *120*, 421–433.

Cowell, R.M., Plane, J.M., and Silverstein, F.S. (2003). Complement activation contributes to hypoxic-ischemic brain injury in neonatal rats. J. Neurosci. *23*, 9459–9468.

Dalmau, I., Finsen, B., Zimmer, J., Gonzalez, B., and Castellano, B. (1998). Development of microglia in the postnatal rat hippocampus. Hippocampus *8*, 458–474.

Dangond, F., Hwang, D., Camelo, S., Pasinelli, P., Frosch, M.P., Stephanopoulos, G., Stephanopoulos, G., Brown, R.H., Jr., and Gullans, S.R. (2004). Molecular signature of late-stage human ALS revealed by expression profiling of postmortem spinal cord gray matter. Physiol. Genomics *16*, 229–239.

Fiske, B.K., and Brunjes, P.C. (2000). Microglial activation in the developing rat olfactory bulb. Neuroscience *96*, 807–815.

Fonseca, M.I., Kawas, C.H., Troncoso, J.C., and Tenner, A.J. (2004). Neuronal localization of C1q in preclinical Alzheimer's disease. Neurobiol. Dis. *15*, 40–46.

Gasque, P. (2004). Complement: a unique innate immune sensor for danger signals. Mol. Immunol. *41*, 1089–1098.

Gasque, P., Singhrao, S.K., Neal, J.W., Wang, P., Sayah, S., Fontaine, M., and Morgan, B.P. (1998). The receptor for complement anaphylatoxin C3a is expressed by myeloid cells and nonmyeloid cells in inflamed human central nervous system: analysis in multiple sclerosis and bacterial meningitis. J. Immunol. *160*, 3543–3554.

Hirai, H., Pang, Z., Bao, D., Miyazaki, T., Li, L., Miura, E., Parris, J., Rong, Y., Watanabe, M., Yuzaki, M., and Morgan, J.I. (2005). Cbln1 is essential for synaptic integrity and plasticity in the cerebellum. Nat. Neurosci. *8*, 1534–1541.

Hooks, B.M., and Chen, C. (2006). Distinct roles for spontaneous and visual activity in remodeling of the retinogeniculate synapse. Neuron *52*, 281–291.

Howell, G.R., Libby, R.T., Marchant, J.K., Wilson, L.A., Cosma, I.M., Smith, R.S., Anderson, M.G., and John, S.W. (2007). Absence of glaucoma in DBA/2J mice homozygous for wild-type versions of Gpnmb and Tyrp1. BMC Genet. *8*, 45.

Hua, J.Y., and Smith, S.J. (2004). Neural activity and the dynamics of central nervous system development. Nat. Neurosci. *7*, 327–332.

Huberman, A.D. (2007). Mechanisms of eye-specific visual circuit development. Curr. Opin. Neurobiol. *17*, 73–80.

Huh, G.S., Boulanger, L.M., Du, H., Riquelme, P.A., Brotz, T.M., and Shatz, C.J. (2000). Functional requirement for class I MHC in CNS development and plasticity. Science *290*, 2155–2159.

Jaubert-Miazza, L., Green, E., Lo, F.S., Bui, K., Mills, J., and Guido, W. (2005). Structural and functional composition of the developing retinogeniculate pathway in the mouse. Vis. Neurosci. *22*, 661–676.

Jennings, C. (1994). Developmental neurobiology. Death of a synapse. Nature *372*, 498–499.

John, S.W., Anderson, M.G., and Smith, R.S. (1999). Mouse genetics: a tool to help unlock the mechanisms of glaucoma. J. Glaucoma *8*, 400–412.

Johnson, S.A., Pasinetti, G.M., and Finch, C.E. (1994). Expression of complement C1qB and C4 mRNAs during rat brain development. Brain Res. Dev. Brain Res. *80*, 163–174.

Katz, L.C., and Shatz, C.J. (1996). Synaptic activity and the construction of cortical circuits. Science *274*, 1133–1138.

Libby, R.T., Anderson, M.G., Pang, I.H., Robinson, Z.H., Savinova, O.V., Cosma, I.M., Snow, A., Wilson, L.A., Smith, R.S., Clark, A.F., and John, S.W. (2005). Inherited glaucoma in DBA/2J mice: pertinent disease features for studying the neurodegeneration. Vis. Neurosci. *22*, 637–648.

Maslinska, D., Laure-Kamionowska, M., and Kaliszek, A. (1998). Morphological forms and localization of microglial cells in the developing human cerebellum. Folia Neuropathol. *36*, 145–151.

Mastellos, D., and Lambris, J.D. (2002). Complement: more than a 'guard' against invading pathogens? Trends Immunol. *23*, 485–491.

Meyer-Franke, A., Kaplan, M., Pfrieger, F., and Barres, B. (1995). Characterization of the signaling interactions that promote the survival and growthof developing retinal ganglion cells in culture. Neuron *15*, 805–819.

Micheva, K.D., and Smith, S.J. (2007). Array tomography: a new tool for imaging the molecular architecture and ultrastructure of neural circuits. Neuron *55*, 25–36.

Mitchell, D.A., Kirby, L., Paulin, S.M., Villiers, C.L., and Sim, R.B. (2007). Prion protein activates and fixes complement directly via the classical pathway: implications for the mechanism of scrapie agent propagation in lymphoid tissue. Mol. Immunol. *44*, 2997–3004.

Morgan, B.P., and Gasque, P. (1996). Expression of complement in the brain: role in health and disease. Immunol. Today *17*, 461–466.

Muller, C.M., and Best, J. (1989). Ocular dominance plasticity in adult cat visual cortex after transplantation of cultured astrocytes. Nature *342*, 427–430.

Nauta, A.J., Bottazzi, B., Mantovani, A., Salvatori, G., Kishore, U., Schwaeble, W.J., Gingras, A.R., Tzima, S., Vivanco, F., Egido, J., et al. (2003). Biochemical and functional characterization of the interaction between pentraxin 3 and C1q. Eur. J. Immunol. *33*, 465–473.

Nilsson, L.G., Sikstrom, C., Adolfsson, R., Erngrund, K., Nylander, P.O., and Beckman, L. (1996). Genetic markers associated with high versus low performance on episodic memory tasks. Behav. Genet. *26*, 555–562.

Prasad, S.S., and Cynader, M.S. (1994). Identification of cDNA clones expressed selectively during the critical period for visual cortex development by subtractive hybridization. Brain Res. *639*, 73–84.

Ritch, R., Shields, M.B., and Krupin, T. (1996). The Glaucomas: Clinical Science, Second Edition (St Louis, MO: Mosby-Year Book).

Sahu, A., and Lambris, J.D. (2000). Complement inhibitors: a resurgent concept in anti-inflammatory therapeutics. Immunopharmacology *49*, 133–148.

Sanes, J.R., and Lichtman, J.W. (1999). Development of the vertebrate neuromuscular junction. Annu. Rev. Neurosci. *22*, 389–442.

Schaeren-Wiemers, N., and Gerfin-Moser, A. (1993). A single protocol to detect transcripts of various types and expression levels in neural tissue and cultured cells: in situ hybridization using digoxigenin-labelled cRNA probes. Histochemistry *100*, 431–440.

Schiefer, J., Kampe, K., Dodt, H.U., Zieglgansberger, W., and Kreutzberg, G.W. (1999). Microglial motility in the rat facial nucleus following peripheral axotomy. J. Neurocytol. *28*, 439–453.

Selkoe, D.J. (2002). Alzheimer's disease is a synaptic failure. Science *298*, 789–791.

Singhrao, S.K., Neal, J.W., Rushmere, N.K., Morgan, B.P., and Gasque, P. (2000). Spontaneous classical pathway activation and deficiency of membrane regulators render human neurons susceptible to complement lysis. Am. J. Pathol. *157*, 905–918.

Stasi, K., Nagel, D., Yang, X., Wang, R.F., Ren, L., Podos, S.M., Mittag, T., and Danias, J. (2006). Complement component 1Q (C1Q) upregulation in retina of murine, primate, and human glaucomatous eyes. Invest. Ophthalmol. Vis. Sci. *47*, 1024–1029.

Steele, M.R., Inman, D.M., Calkins, D.J., Horner, P.J., and Vetter, M.L. (2006). Microarray analysis of retinal gene expression in the DBA/2J model of glaucoma. Invest. Ophthalmol. Vis. Sci. *47*, 977–985.

Torborg, C.L., and Feller, M.B. (2004). Unbiased analysis of bulk axonal segregation patterns. J. Neurosci. Methods *135*, 17–26.

Ullian, E.M., Sapperstein, S.K., Christopherson, K.S., and Barres, B.A. (2001). Control of synapse number by glia. Science *291*, 657–661.

Wang, J.T., Kunzevitzky, N.J., Dugas, J.C., Cameron, M., Barres, B.A., and Goldberg, J.L. (2007). Disease gene candidates revealed by expression profiling of retinal ganglion cell development. J. Neurosci. *27*, 8593–8603.